Chemical Engineering Journal 322 (2017) 224–233

Contents lists available at ScienceDirect

Chemical Engineering Journal

journal homepage: www.elsevier.com/locate/cej

Development of a selective electrodialysis for nutrient recovery and desalination during secondary effluent treatment

Rudong Liu, Yunkun Wang *, Gang Wu, Jiening Luo, Shuguang Wang

Shandong Key Laboratory of Water Pollution Control and Resource Reuse, School of Environmental Science and Engineering, Shandong University, Jinan 250100, China

HIGHLIGHTS

- A selective electrodialysis reactor was developed for nutrients recovery and desalination.
- HPO_4^{2-} and NO_3^- were separated and concentrated in different compartments of the SED system.
- The simultaneous removal of Cl^-, NO_3^- and HPO_4^{2-} indicated a well desalination performance.
- A mathematics model was developed to simulate the variation of current.

GRAPHICAL ABSTRACT

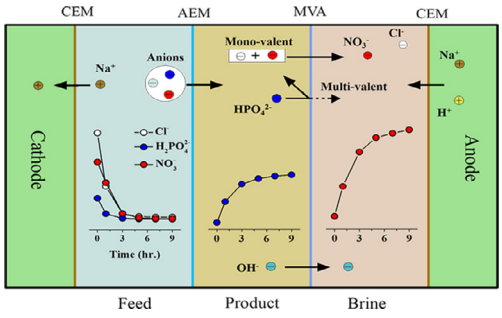

ARTICLE INFO

Article history:
Received 1 January 2017
Received in revised form 3 March 2017
Accepted 31 March 2017
Available online 5 April 2017

Keywords:
Selective electrodialysis
Secondary wastewater effluents
Nutrients recovery
Desalination

ABSTRACT

Recovering resources, especially nutrients and water, from biologically treated secondary effluent, which in line with the concept of zero liquid discharge, has attracted increasing interests. In this study, a selective electrodialysis (SED) was developed to separate and recover the nitrogen and phosphorus nutrients and enforce desalination during secondary effluents treatment under low applied voltages. The SED system performance as well as current efficiency and energy consumption were investigated under different number of ion exchange membrane trios, applied voltages and flow rates. Nitrate could be reconcentrated to 40.64 mg-N L^{-1} in brine compartments while the phosphate was retained by a monovalent anion exchange membrane and concentrated to 21.2 mg-P L^{-1} in product compartments. The conductivities of feed compartments were all below 2 μS/cm after treatment, indicating a well desalination performance of the SED system. The current efficiency was obtained to be lower under a higher voltage, and a mathematical fitting of current was developed to confirm the existence of water dissociation under higher voltages. The SED with more ion exchange membrane trios proved to be able to perform an effective desalination under advantageous electricity consumption conditions. With the capability to reconcentrate nutrients and simultaneously realize zero liquid discharge of secondary wastewaters, the examined SED treatment technology has a potential for practical nutrient recovery and sustainable water reuse.

© 2017 Elsevier B.V. All rights reserved.

1. Introduction

The biologically treated secondary effluent from existing wastewater treatment plants still contain a certain amount of nutrients (such as NO_3^- and HPO_4^{2-}) [1] and salinity (such as Na^+, Ca^{2+}, K^+, Mg^{2+} and Cl^-). The insufficient treatment could lead to eutrophication [2] and influence the reuse of reclaimed water [3]. Moreover, the phosphorous is an important mineable resource [4], recovering P from wastewater streams for reuse can alleviate the problem of limited phosphate resource supply [5]. However the zero discharge of N and P remains to be a tough problem with the currently used techniques, such as activated sludge and anaer-

* Corresponding author.
E-mail address: ykwang@sdu.edu.cn (Y. Wang).

http://dx.doi.org/10.1016/j.cej.2017.03.149
1385-8947/© 2017 Elsevier B.V. All rights reserved.

obic/anoxic/oxic processes, especially along with the increasingly stringent effluent standards. Moreover, these biological treatment technologies are less effective to reduce salinity [1]. In light of these problems, novel wastewater treatment processes capable of removing and recovering N and P resources as well as reducing salinity to realize the zero liquid discharge (ZLD) of secondary effluents are necessary to develop to satisfy the increasing need of environment protection [1,6,7].

In recent years, ZLD technology has been utilized in wastewater treatment to eliminate liquid waste and maximize water usage efficiency [8]. Several techniques are available to remove and recover nutrients from secondary wastewaters, such as chemical precipitation, adsorption and membrane filtration [9]. Among these technologies, the chemical precipitation is applied as an efficient process by using Fe or Al salts [10]. However the generated residues need further disposal [11] and this method is less effective to reduce salinity. The high salinity in wastewater as well as high regeneration costs would limit the widely application of adsorption.

Recently, membrane filtration technologies, such as reserve osmosis (RO), nanofiltration (NF) and electrodialysis (ED), have drawn much attention to desalinize and recover useful materials in wastewater treatment [12–14]. Pressure membrane processes like RO and NF need a quite complex pretreatment to alleviate the membrane fouling [15,16], resulting in needless capital cost and energy consumption. Furthermore, the RO is ion uncontrollable and highly relying on the size of molecules [17]. However, as an electrochemical membrane separation process [18,19], ED is capable of separating undesired ions from wastewaters more energy-efficient [18,21] with an applied electric filed [20,21] as the driving force [22] to get a higher water recovery [17]. ED would be an alternative technique in an environmental and economical manner to realize the ZLD and nutrients recovery during secondary effluent treatment.

Previous studies of ED were focused on the treatment of wastewaters for demineralization and water reclamation [20,21]. As the ions migrated through the ion exchange membranes (IEMs) to concentrate in another compartment of ED, the unique ion separation mechanism provided a selective method for nutrient recovery [22,23]. ED could selectively generate high quality nutrient products [24], like ammonia and phosphorus enrichment were observed from urine and other wastewaters [25–27]. Simultaneous recovery of ammonia and phosphorus was achieved via the integration of ED with struvite reactor [2], and ED was also integrated with bio-electrochemical system to recover resources [28]. In desalination often multi ionic compositions are encountered, but the conventional ED could not separate ions of the same charge but different valence. The use of selective IEMs brought appreciable separation efficiencies between different valent ions [29]. Simultaneous phosphate removal and separately reconcentration against chloride were achieved by using the selective IEMs [30,31]. ED also enjoys the important advantage for small to medium sized applications where high quality product is required [32]. Although substantial researches have been published on the subject of electrodialysis over the past decades, little information is available about the application of ED in nutrients separation and recovery from low concentration wastewaters like biological treated secondary effluent.

In this study, by integrating monovalent anion exchange membrane (MVA) into a conventional ED, a novel selective electrodialysis (SED) reactor was developed for secondary effluent desalination and nutrient recovery. As an alternative of ZLD procedure, the potential application of this technology in N and P resource removal and separately recovery was evaluated. The performances of SED in terms of nitrate and phosphate separation and recovery as well as desalination were studied under different IEM trios, flow rates and voltages. The selectivity of MVA, the current efficiencies of different ions and the variation of pH in different compartments were evaluated under different voltages. A mathematical fitting of current was developed to compare with the monitored current, which verify the water dissociation under higher voltages. The results of this study would provide a novel process for resources recovery during secondary effluent treatment.

2. Materials and methods

2.1. Reactor construction

The assembled ED reactor was constructed as shown in Fig. 1. Two electrodes were titanium electrodes coated ruthenium (Dexin Taiye, China). A stack of IEMs (Neosepta, Astom Co., Japan) were placed between the anode and the cathode compartments, and their properties were listed in Table 1. From anode to cathode, a cation exchange membrane (CEM), an anion exchange membrane (AEM), a MVA and an extra CEM were placed in order. The effective area of an IEM was 25 cm^2. The neighboring membranes were separated with a thickness of 1 mm by using the plastic gaskets, creating three compartments, which were denoted as feed, product and brine compartment, respectively. An electrochemical worksta-

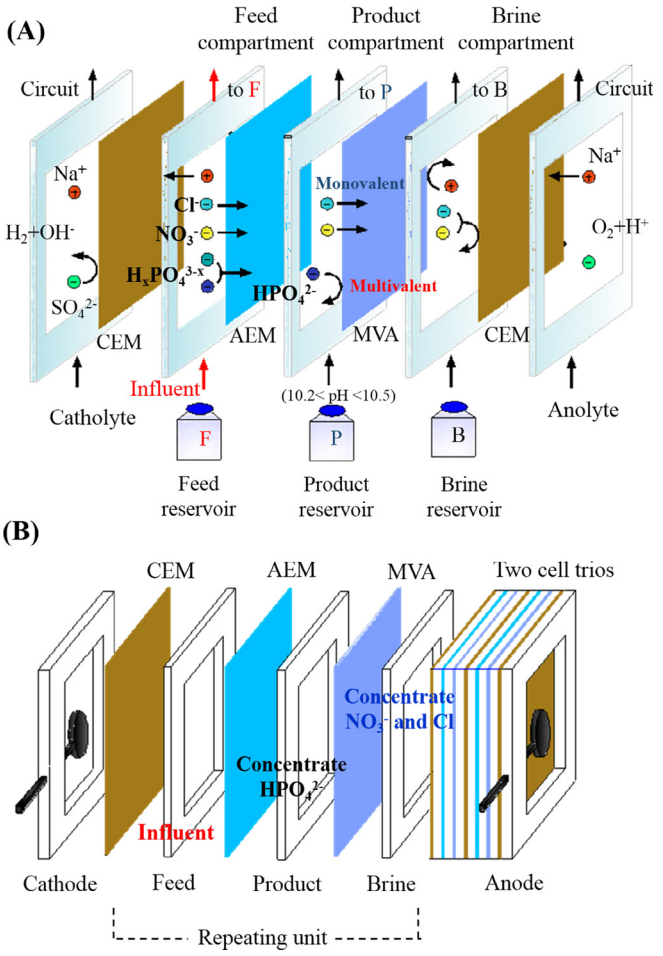

Fig. 1. (A) Single membrane-trio ED reactor schematic design for treatment of secondary effluent. (CEM: cation exchange membrane; AEM: anion exchange membrane; MVA: monovalent anion exchange membrane.) The experiment was ran in a batch mode, and the three different streams are pumped from the reservoirs. The shown arrows indicate the migrating direction of different ions (B) 3 membrane-trios schematic design. The electrodes are two titanium electrodes coated with a ruthenium mixed metal oxide.

Table 1
Main Characteristics of Membranes Used in the Experiments.

	Membrane type	Thickness (mm)	Area resistance ($\Omega \cdot cm^2$)	Burst strength (MPa)	Permselectivity	Maximum temperature (°C)
CEM	Neosepta CMX	0.17	3.0	≥0.40	>0.9	40
AEM	Neosepta AMX	0.14	2.4	≥0.25	>0.9	40
MVA	Neosepta ACS	0.13	3.8	≥0.15	>0.9	40

tion (CHI 660E, Chenhua, China) was used to maintain constant voltages throughout the experiments.

A membrane trio (CEM, AEM and MVA) formed a three-compartment (denoted as feed, product and brine compartment, respectively) configuration as mentioned above. A three IEM trios stack was constructed and sandwiched between the electrodes compartments to shape a thicker reactor. During the operation, the feed solution flowed continuously through each feed cell as the detailed flow direction in the IEMs stack (Fig. 1), meanwhile, the product and brine streams followed the same schemes with the feed cell in the stack which is shown in Fig. 1.

2.2. The synthetic secondary wastewater preparation

The synthetically simulated secondary effluent (feed stream) and the initial solution composition of other streams were shown in Table 2. 10 mM NaCl was added in feed solution as the typical salt contents to emulate the desalination process of secondary effluent. All salts used in this study were analytical grade bought from Sinopharm Group Co. Ltd, and the salts were all dissolved in deionized water.

2.3. Reactor operation

During the experiments, the SED was operated in a recirculating batch mode. Three plastic bottles were employed as feed, product and brine tanks, and the three external solutions are pumped circularly from the tanks respectively through the ED stack, and the flow rates of IEM stacks and electrode rinsing solutions were equal and uniform to avoid hydrostatic pressure differences. The pH in the product compartment was adjusted to 10.2–10.5 by adding 0.5 M NaOH throughout the operation to improve MVA selectivity toward HPO_4^{2-}, which accounted for approximately 99% of the phosphate at this range of pH. When applying an electric field, anions and cations from the solution are attracted toward the anode and cathode, respectively. Thus, the monovalent anions, chloride and nitrate in feed compartment go through the AEM, product compartment and MVA in sequence to concentrate in brine compartment while the multivalent phosphate in feed compartment goes through the AEM and was retained by the MVA to concentrate in the product compartment.

The SED was operated in a constant voltage mode because a much higher voltage across the stack would not develop as the current decreased when the dilute concentration was very low. A series of preliminary experiments with different concentrations of NaCl solutions and flow rates (4–16 mL/min) were conducted (Fig. S1). The variable voltages were set to 3 V, 5 V and 7 V with single-trio IEM in the stack as a further increase of the applied voltage results only in a small increase of current between 3 V and 5 V where limiting current happened, and the current increases again at 7 V. The flow rates were set to 8 and 16 mL/min as the current increased vastly at this range of voltages. As more IEM stacks bring the wider spacing between electrodes and greater system resistances [28], the applied voltages should be enlarged, and the voltages were 9 V and 15 V with 3-trio IEMs. Since the current efficiency strongly decreases due to the increasing in the resistance of the dilute solution and the operating time of each experiment was determined by an occasion when the monitored conductivity of feed compartment was reduced to 2 μS/cm [33].

Table 2
Initial Feed, Product, Brine and Electrode Solution Used in the Experiments.

	Content	Concentration	Volume
Feed	NaCl	355 mg-Cl L^{-1}	250 mL
	$NaNO_3$	30 mg-N L^{-1}	
	Na_2HPO_4	10 mg-P L^{-1}	
Product & Brine	NaCl	355 mg-Cl L^{-1}	100 mL
Electrode Solution	Na_2SO_4	1420 mg L^{-1}	200 mL

2.4. Measurement and data processing

In the experiments, the current was monitored and recorded by the electrochemical workstation. The three compartments were sampled and analyzed for pH (PHS-3C, Inesa Instrument, China) and conductivity (DDS-307A, Inesa Instrument, China) at a certain time interval. The concentrations of chloride, phosphate and nitrate were determined by ion chromatography (ICS-900 Ion Chromatography, DIONEX, USA).

2.4.1. Recovery efficiency and recovery rate

The nutrient recovery efficiency was defined as the ratio of the amount of phosphate in product or nitrate in brine compartment to the total content of phosphate or nitrate in the feed. The recovery rate was defined as the increase in the amount of phosphate in product or nitrate in brine compartment per unit time.

2.4.2. Current efficiency

One purpose of the fractioning ED stack is to remove the nutrient ions. Therefore, the current efficiency (CE) of ion i (negative charge) of ED was calculated as [34,35]:

$$\eta = \frac{Q_i}{Q_{applied}} \tag{1}$$

$$Q_i = \frac{|Z_i| \cdot F \cdot \frac{\Delta m_i(t)}{M_i}}{N} \tag{2}$$

$$Q_{applied} = \int_0^t Idt \tag{3}$$

Where Q is the electric quantity; $\Delta m_i(t)$ is the weight change of ion i in the target compartment; M_i is the molar mass of ion i; Z_i is the charge of ion i; F is the Faraday constant; I is recorded current; t is the overall operating time of a batch experiment; N is the number of cell trios in the ED stack.

2.4.3. Selectivity

The selectivity of membranes between ion A and B (S_B^A) was calculated as follows [36]:

$$S_B^A = \frac{t_A}{t_B} \cdot \frac{C_B}{C_A} = \frac{J_A \cdot C_B}{J_B \cdot C_A} \tag{4}$$

$$t_A = \frac{J_A}{\sum J_i} \tag{5}$$

Where C is the concentration of the ions on the dilute side of membrane; t is the transport number of the ion through the membrane; J is the flux of ions through the membrane.

2.4.4. Energy Consumption (EC)

The energy consumption of the ED process can be calculated as:

$$EC = \frac{U \cdot \int_0^t Idt}{\beta \cdot V_f} \quad (6)$$

where U is the applied voltage; V_f is the initial volume of the feed solution, $\beta = 3.6 \cdot 10^6$ kWh/J (note: these numbers do not include pumping energy).

2.4.5. Mathematical fitting of current

Once the operating voltage was applied, the total current is the sum of electric current carried by each electrolyte correspondingly. Hereafter, the mathematical fitting is proposed assuming that the system contains n kinds of electrolytes, and the electric current of *ith* electrolyte is obtained from the flux that flows through the *ith* circuit [35], which is given by:

$$\mathrm{I} = \sum I_i \quad (7)$$

$$I_i = F \cdot J_i \cdot M_s \cdot |Z_i| \quad (8)$$

where I_i and J_i are the electric current and flux of *ith* electrolyte, M_s is effective area of ion exchange membrane. The ionic flux through the IEM within a time interval can be calculated using the equation [37]:

$$J_i = \frac{(C_i^{t_1} - C_i^{t_2}) \cdot V_f}{M_s \cdot N \cdot t} \quad (9)$$

where C_i and t are ion concentration and time period between t_1 to t_2, respectively.

3. Results and discussion

3.1. Desalination of the single-trio IEM reactor

As mentioned above, ZLD is used to eliminate the liquid waste and recover the majority of water for reuse [8]. In this research, SED was applied to remove the inorganic salts to achieve the ZLD in secondary effluent. Under different external voltages, the concentration changes of Cl^-, NO_3^- and HPO_4^{2-} in three compartments were evaluated with a flow rate of 8 mL/min (Figs. 2 and 3), and the conductivities of solutions in different compartments were monitored (Fig. 2). For ZLD concept in this study, the highest possible removal of salts was achieved as the conductivity of feed solution reaching 2 μS/cm at the end of the ED, indicating a well desalination performance that almost all inorganic ions were removed. As the IEMs on both sides of product compartment were ideal anion exchange membranes, the concentration of Na^+ in the product stream remained unchanged, parts of Cl^- remained in product compartment due to the electroneutrality effect (Fig. 2A and B) [38], but at 7 V, the concentration of Cl^- decreased as the OH^- generated by water dissociation participated in the migration into product compartment owing to the strong electric field.

The desalination of SED remained the same, nearly, at a fixed volume and flow rate, and the conductivities dropped faster and less time would be taken with a bigger voltage like previous researches reported [4]. However, the fast desalination rate did not mean an increased current efficiency. In this research, an overall CE_{Cl}^- in feed compartment of 71.1% and 74.2% were obtained under 3 V and 5 V, and then decreased to 43.7% under 7 V, which should be attributed to the possible water dissociation took place under high voltages [39]. Different from widely high salinity aqueous phases used in conventional ED, the synthetic secondary wastewater used in this experiment was very dilute, the water dissociation phenomenon could not be avoided to get the well desalination performance. So, in our future study, some feasible measures can be used to reduce the water dissociation, such as introduced ion exchange resin into SED to increase the conductivity to form the electrodeionization [40].

3.2. Nitrate and phosphate separations and recoveries

ED has been widely used for salts recovery in aqueous phases, but the separation of mono- and multi-valent ions is quite a tough problem. As shown in Fig. 3, the nutrient ions became dilute in feed compartments while the nitrate and phosphate (calculation with nitrogen and phosphorus element, following the same) concentrated in the brine and product compartments, respectively. We can see that nearly all nitrate and phosphate in the diluted compartment could be removed under each condition. Nitrate (initially 26.2 mg-N/L in feed) was concentrated by a factor of 1.55 to a maximum concentration of 40.64 mg-N/L (E = 5 V, single-IEM, trio) (Fig. 3B) in brine compartment, and the overall recovery rate was 2.27 mg-N L^{-1} h^{-1}. Similarly, phosphate (initially 9.78 mg-P/L in feed) was reconcentrated to 21.2 mg-P/L in product chamber with a rate of 1.13 mg-P L^{-1} h^{-1} (E = 5 V, single-IEM, trio) (Fig. 3E). Correspondingly, the recovery efficiency of N in brine solution and P in product solution were 62.1% and 86.5%, respectively (E = 5 V, single-IEM, trio). Meanwhile, when the voltage was 3 V, the recovery efficiency of N and P were 67.2% and 77.4%, respectively, and the corresponding recovery rates were 1.75 mg-N L^{-1} h^{-1} and 0.767 mg-P L^{-1} h^{-1} (E = 3 V, single-IEM, trio). So, the recovery rate increased as the processing capacity of the IEM stack increased with the increasing applied voltage (Fig. 3) [4]. Apart from the higher recovery rate and the shorter operating time, the recovery efficiencies of nitrate and phosphate under 5 V was higher than that of 3 V (Fig. 3). However, the phosphate permeated to the brine compartment at 7 V (Fig. 3C) which indicated that a much higher voltage might bring negative effects.

Fig. S2 illustrated variations of pH in three tanks under different operating voltages. A more intensive water dissociation near the membrane took place under a higher voltage as the H^+ generated in the feed compartment resulting in a lower pH value (E = 5 V, pH < 6 and E = 7 V, pH < 4). Although the pH in product tanks is stable (about 10.2–10.5) as a result of NaOH dosing for pH adjustment, the concentration of H^+ increased at the MVA membrane/solution interface by water dissociation at 7 V. The occurrence of phosphate migrated into brine compartment was due to parts of HPO_4^{2-} inside the diffusion boundary layer near MVA surface turned to $H_2PO_4^-$.

3.3. Effect of flow rate

The flow rates together with the applied high voltages are responsible for occurrence of concentration polarization owing to the existence of boundary layers near the membrane surfaces. The effect of flow rate of SED at 5 V and 7 V was investigated. As demonstrated in Table 3, the operating time decreased from 12 h to 7.5 h at 7 V with a greater flow rate, the desalination of SED remained nearly the same with a fixed flow rate, and the phosphate recovery was improved. Magnifying the flow rates can better mixing the dilute solution to decrease the thickness of the boundary layers to enhance the transfer of the ions [41]. As illustrated in Fig. 4, the specific ion remaining versus feed solution conductivity were monitored at different flow rates and samples were adopted with same time interval. Analyzing Fig. 4A and B one finds that ions were removed at a much higher rate with a greater flow rate at 7 V. The conductivity decreased slower than ion migration at 8 mL/min

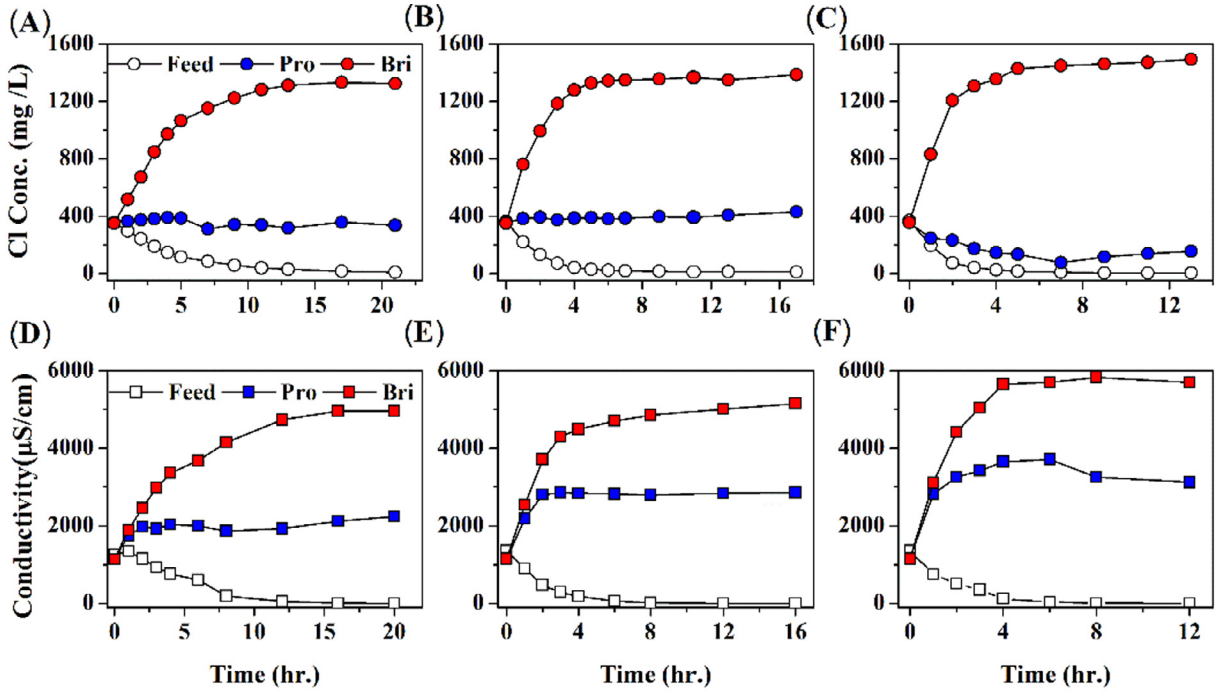

Fig. 2. Effects of voltage on the desalination of single membrane-trio ED reactor as a function of time (Feed: feed compartment; Pro: product compartment; Bri: brine compartment). The initial concentration of Cl was 355 mg/L, the flow rate was 8 mL/min. (A), (B) and (C) are the concentration curve of Cl when the voltage was 3 V (Feed = 250 mL, Pro & Bri = 100 mL; 21-h operation), 5 V (17-h operation) and 7 V (13-h operation), respectively. (D), (E) and (F) are the conductivity curve of three compartments under three voltages.

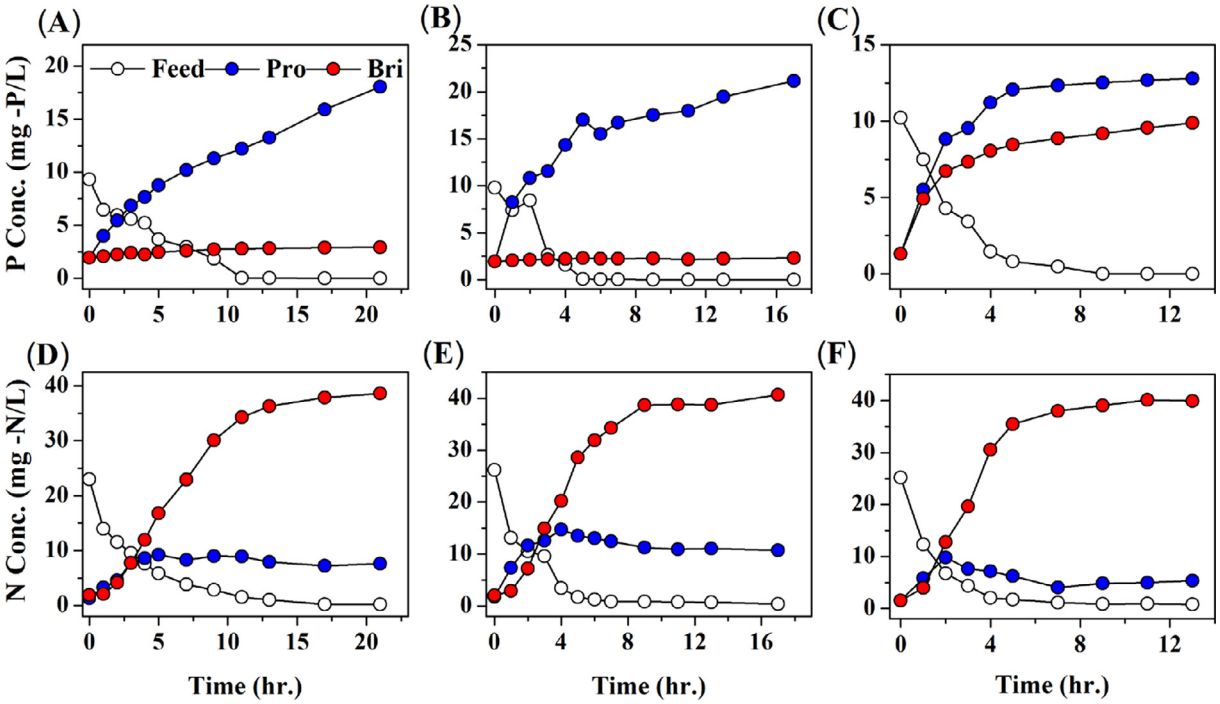

Fig. 3. Effects of voltage on the separations and recoveries of N and P as a function of time. The flow rate was 8 mL/min (A), (B) and (C) are the concentration curve of P at 3 V, 5 V and 7 V, respectively. (D), (E) and (F) are the concentration curves of N under three voltages.

owing to the concave curve, which indicated OH^- generate by water dissociation was the composition of solution conductivity, and the water dissociation got limited for the linear relation at 16 mL/min. Moreover, the consumed electricity was reduced and the overall current efficiency (CE) increased from 53.9% to 71.7% as the flow rate increased to 16 mL/min (Fig. 4D), and the CE of 84% was achieved at 5 V. Furthermore, one of the interesting occurrences was the monovalent ions were removed at a much higher rate than divalent ions as the removal efficiency of monovalent ions was larger (Fig. 4) [22]. The initial concentration gradient of

Table 3
The performance of single-trio IEM experiment with different voltages and flow rates.

Voltage (V)	Flow rate (mL/min)	Operation time (h)	Mass balance (%)					
			N			P		
			Feed	Pro	Bri	Feed	Pro	Bri
3 V	8	21	3.3	13.2	67.2	0.2	77.4	12.6
5 V	8	16	0.1	16.4	62.1	0.1	86.5	9.5
	16	11	0.1	10.5	73.9	0	85.4	8.4
7 V	8	12	0.2	8.6	63.4	0	50.1	38.6
	16	7.5	0.1	6.6	74.5	0	75.4	16.6

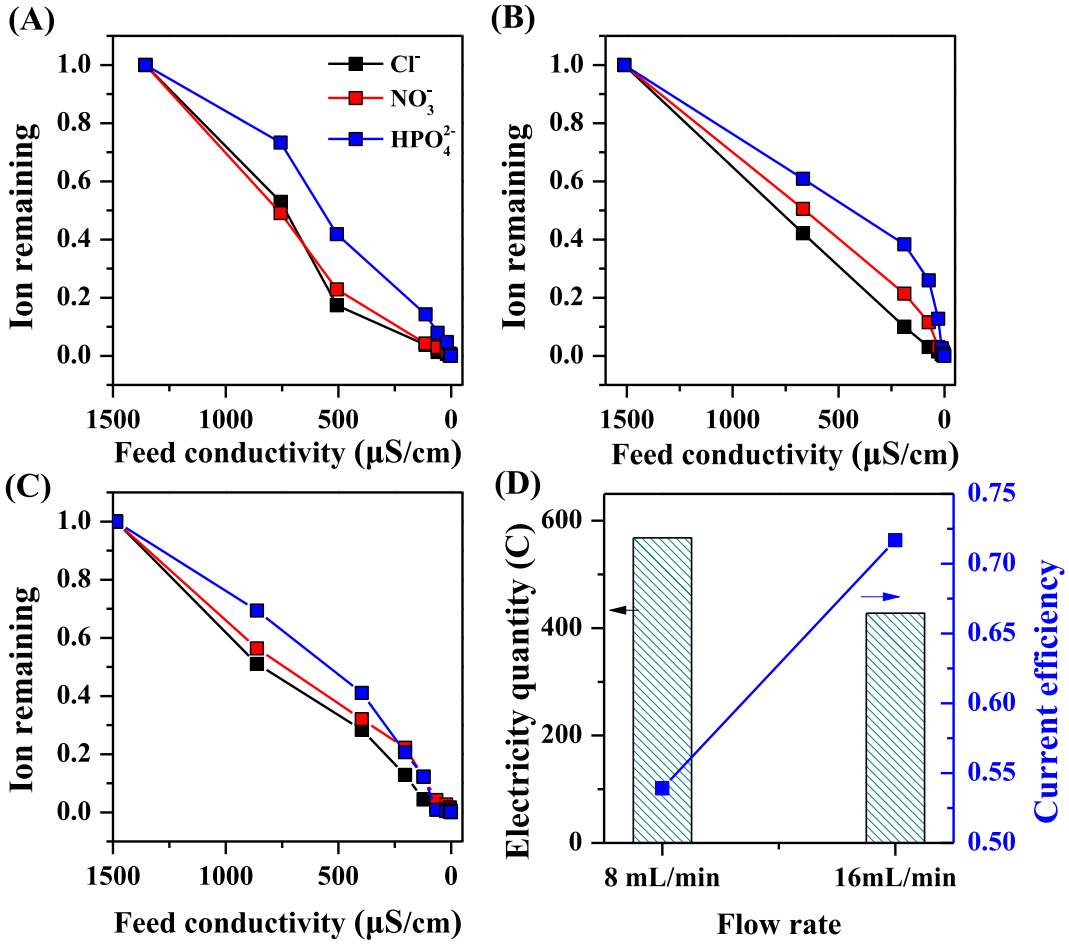

Fig. 4. Measured remaining ions ratios (%) in the feed solution monitored with feed conductivity during desalination of (A) 5 V at 8 mL/min; (B) and (C) 7 V at 8 and 16 mL/min, respectively. (D) the consumed electricity quantity and current efficiency at 7 V with different flow rates.

P across the AEM was minor to N. Moreover, as shown in Table S3, phosphate has relatively small values of the ionic conductivity compared to nitrate. Thus, the phosphate migrated slower than nitrate, and the bigger radius of phosphate might attribute to the slow migration inside the membrane. Consequently, the recovery rate of P decreased under lower voltages, and the part of P absorbed by IEM desorbed slowly as the current decreased along with time resulting in the slow rising trend instead of reaching a stable-state (Fig. 2A and B).

3.4. The MVA selectivity and current fitting

In this study, nitrate and phosphate were separated and recovered by using the MVA. As illustrated in Fig. 5, the MVA had a high selectivity toward nitrate at first for the $S_P^N > 1$ at the initial stage of all three different voltages. However, the MVA selectivity decreased gradually as time elapsed. During the operation, the HPO_4^{2-} were retained in product compartment to create a relatively high concentration gradient across the MVA, at the same time, the high concentration of nitrate and chloride in brine compartment. The existing concentration difference across the MVA made it easier for HPO_4^{2-} but harder for NO_3^- in product compartment to go through the MVA, resulting in the gradual decrease of S_P^N. Moreover, the firstly accumulation of nitrate in product chamber and the subsequent migration of nitrate to brine chamber might result in the negative $\frac{dC_{NO3^-}}{dt}$ of product compartment in Eq. (6) as well as the appearance of the negative value of S_P^N (E = 3 V, T = 7 h, $S_P^N = -0.78253$; E = 5 V, T = 7 h, $S_P^N = -0.6622$) (Fig. 5).

Since the feed solution became dilute as the ions transferred to the other compartments, the resistance of the system increased

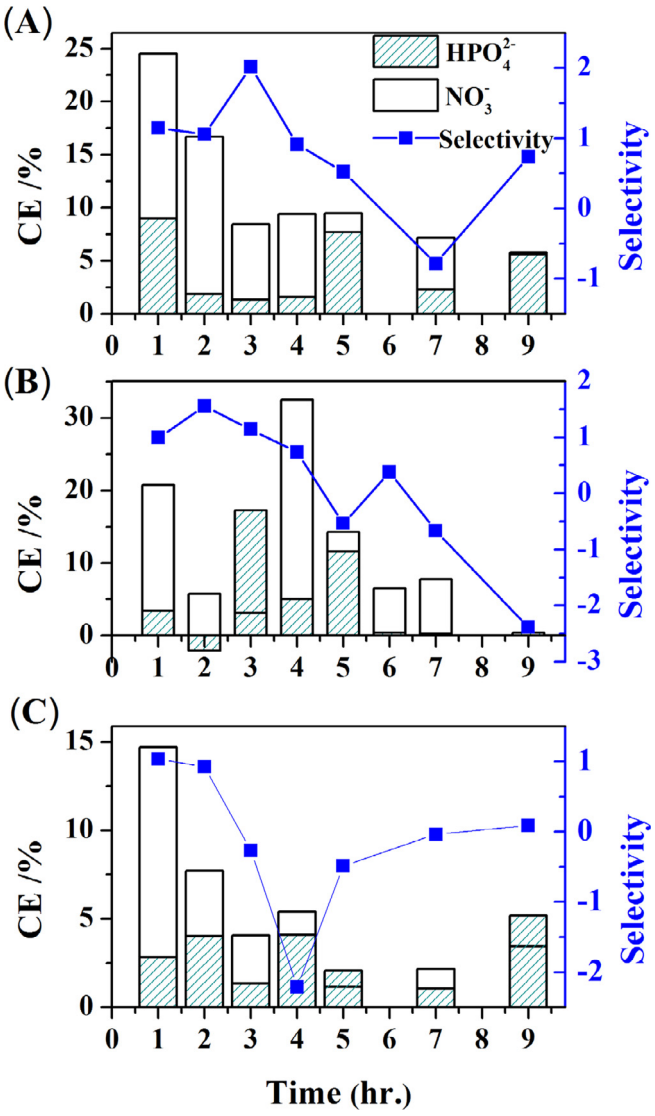

Fig. 5. Performance of ED reactor at different voltages. The flow rate was 8 mL/min. (A), (B), (C), when the voltages were 3 V, 5 V and 7 V, respectively. The columns indicate current efficiency of phosphate and nitrate in feed compartment, and the blue dots refer to the MVA selectivity.

gradually, resulting in the decrease of the relevant current which had been observed in Fig. 6. As the phosphate and nitrate had relatively small values of the ionic contents compared to chloride, the current was mostly generated by the migration of Cl^-. Current efficiencies (CE) of NO_3^- and HPO_4^{2-} in feed compartment were calculated. The CE_{NO3}^- decreased from 24.0% to 5.8% (E = 3 V, single-trio IEM) (Fig. 5A) as a result of the depletion of nitrate. Meanwhile, the CE_{HPO4}^{2-} increased at the first several hours, then dropped to a low value (Fig. 5A and B). The CE_{NO3}^- was larger than CE_{HPO4}^{2-} at the beginning (Fig. 5) due to the higher concentration of NO_3^- (30 mg-N L^{-1}) compared with HPO_4^{2-} (10 mg-P L^{-1}) in stock solution, and phosphate migrated slower than nitrate also resulting in a lower CE_{HPO4}^{2-} at first although the standard AEM had no selectivity to divalent anions.

Although the SED contained the feed, concentrate and electrode streams with respective electric resistances, the electric current is always equal everywhere in the system at a point in time (Fig. S3A). As the AEM in SED were assumed to be ideally permselective, according to Faraday's law of electrolysis [35], the current across the AEM was assumed to consist of Cl^-, NO_3^- and $H_xPO_4^{3-x}$

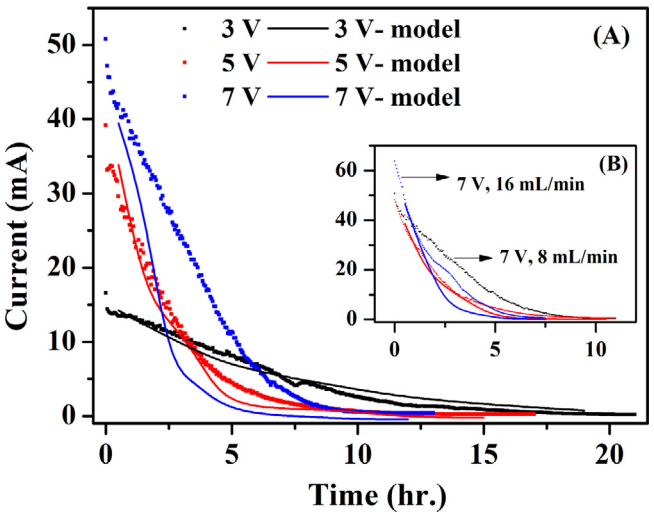

Fig. 6. The variations of monitored current and calculated current in single-trio experiments with (A) the flow rate of 8 mL/min; (B) the flow rate of 16 mL/min.

current [42], which means the sum of migrated current should equal to the recorded current ideally, and the equivalent circuit was shown in Fig. S3B. Here, the electric current through the membrane was mainly determined by the ion flux induced by the externally applied voltage which was discussed in Section 2.4. Fig. 6 demonstrated the changes of monitored current and calculated current with the experimental concentrations under different voltages. When the flow rate was 8 mL/min, we can see that the calculated current was almost consistent with the monitored one under 3 V at first, which confirmed that the higher current efficiency to migrate ions without any side reactions. However, two variations were slightly different from each other as the calculated currents were always higher in the second half of the experiment, which could be attribute to lag effect of the ion flux change owing to the membrane adsorption. The calculated current was always smaller than the monitored one as a result of water dissociation under 5 V, and the discrepancy would be more severe under a higher voltage at 7 V. At higher operating voltages, ions concentration dropped faster, and ions move quicker inside AEM than that in solutions, H^+ and OH^- from water dissociation near the membrane would participate in the ions migration and current generation. Namely, this distinctions proved the existence of water dissociation under higher voltages in Section 3.1, and damages and a short working life of membranes under a higher voltage had been discovered [30]. However, at 16 mL/min, as shown in Fig. 6B, it can be observed that the increase of flow rate determined also the increase of current for the decrease in the resistance, owing to the diminishing of water dissociation by decreasing the boundary layer thickness. However, from a certain point (about 2.5 h), the calculated current was smaller compared to the monitored current at 7 V as the intensive water dissociation happened again for the strong electric filed, which is consistent with the lower current efficiency compared to 5 V. Therefore, selection of a suitable operating voltage is important for an electrodialysis process. Moreover, since limiting current density is proportional to the feed concentration [39] and low salt concentrations is required for the ZLD of secondary wastewaters, the constant voltage mode proved to be a better choice than constant current mode where a more severe water dissociation would happen to maintain the constant generated current. The large membrane areas might be a solution to handle the concentration polarization for a given capacity plant when low salt concentration in a desalination process is required [39].

3.5. Three IEM trios experiment

In a commercial ED system, a series of IEM stacks are alternately spaced in ED system to improve the operation efficiency [22]. In this research, a three IEM trios reactor was constructed. Fig. 7 illustrated the final concentration of anions of the three streams under 9 V and 15 V. As shown in Fig. 7, the chloride decreased in feed compartments to 3.38 and 4.22 mg-Cl L^{-1}, respectively, and were concentrated in brine compartments under 9 V and 15 V (Fig. 7A). Phosphate was reconcentrated to 18.27 and 16.72 mg-P L^{-1} in product compartment under 9 V and 15 V, respectively (Fig. 7B). Similarly, nitrate was concentrated to a maximum concentration of 42.3 mg-N L^{-1} and 37.3 mg-N L^{-1} in brine streams (Fig. 7C). Correspondingly, the recover efficiencies of N and P were 64.28% and 73.67% under 9 V voltage, while they were 56.97% and 67.42% under 15 V.

Fig. 7 showed the dynamic changes of Cl^-, NO_3^- and HPO_4^{2-} in 3-trios IEM experiment under different voltages. When the voltage was 9 V, the removal rate of Cl^- during the first hour was 225.8 mg $L^{-1}h^{-1}$ and decreased to 0.1 mg $L^{-1}h^{-1}$ at the end of the batch (E = 9 V, 3-trios IEM) (Fig. 8A), and the removal rate was higher under 15 V (Fig. 8B) at the beginning resulting from a more intensive ionic migration with a higher voltage. But it is interesting that the concentrate rate of P in product compartment was lower under 15 V and it was supposed that more phosphate went through the MVA as a result of the lower pH value for the more intensive water dissociation happened (Fig. 8B). Notably, the −9 concentration was normalized by the effective area of IEMs (75 cm^2 for 3-trio IEMs and 25 cm^2 for single-trio IEM). Although the reactors with 3-trio IEMs showed higher rates of concentration of nutrients than that with single-trio IEM for the shorter operation time, the N flux was 73.6 mg-N m^{-2} h^{-1} in single-trio IEM experiment (E = 3 V), compared to 62.6 mg-N m^{-2} h^{-1} in 3-trio IEMs experiment (E = 9 V). In addition, the P flux were 34.4 mg-P m^{-2} h^{-1} (E = 3 V, single-trio IEM) and 27.1 mg-P m^{-2} h^{-1} (E = 9 V, 3-trio IEMs), the small stack showed a greater nutrient flux though an individual IEM. Although the electrode reactions occupied parts of applied voltage, the increasing voltage with the increasing number of IEM stacks remains a limitation which would cause resistive losses for water dissociation.

In a SED system, transport of ions to the concentrate compartment depends on the amount of electrical current flowing between the stack. The consumed electricity quantity was calculated by the integration of current with the operational time, and the volumetric energy consumption was obtained by Eq. (7). Fig. 9 showed the conductivity of feed compartment and the corresponding volumetric energy consumption. The vertical dotted lines indicated the point from which little further ion exchange took place as the conductivity in feed compartment was almost constant, and the energy consumptions were 1.456 kWh/m^3 for 3 trios experiment under 9 V and 1.056 kWh/m^3 for single trio experiment under 3 V, which indicated the volumetric energy consumption required for the fractionation was greater as a result of increased resistance with a thicker IEM stack. Fig. 9 also displayed that continuing operation after the indicative points would not lead to a higher energy

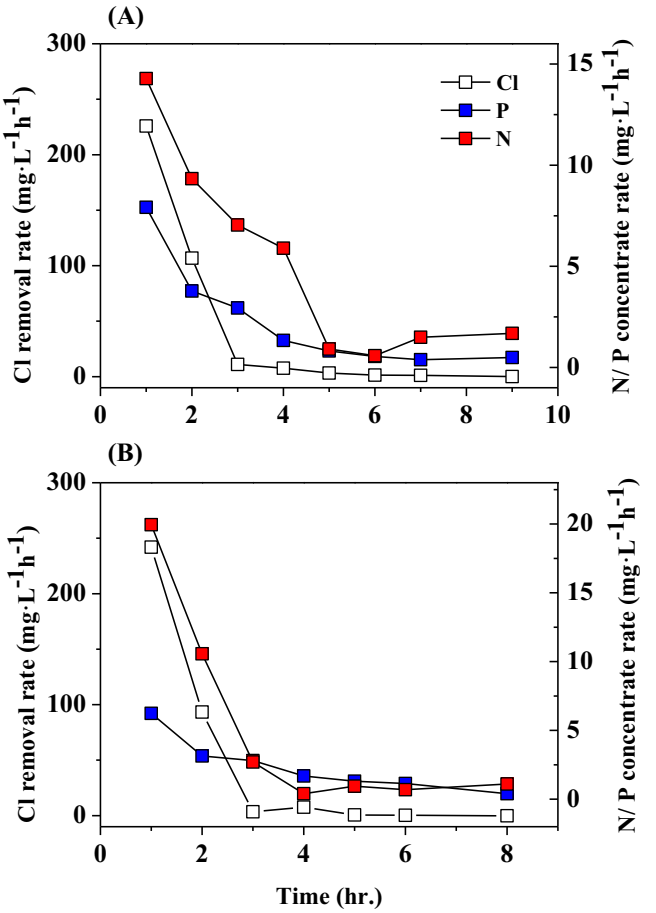

Fig. 8. Effect of voltages on the variation of Cl removal rate, N and P concentrate rate of 3- trios IEM reactor. (A), the voltage was 9 V; (B), the voltage was 15 V.

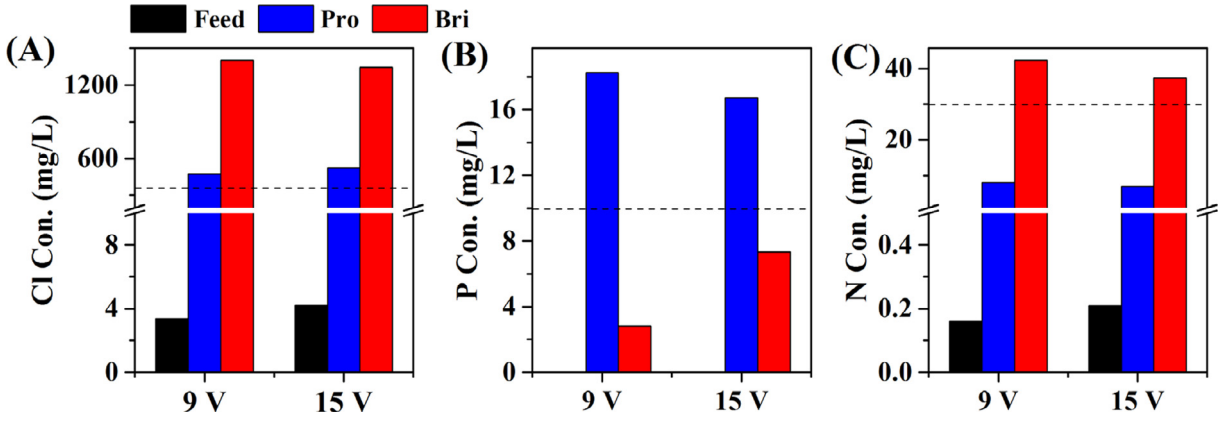

Fig. 7. Effect of voltage on final concentration of (A) chloride, (B) phosphate and (C) nitrate in three compartment of 3-trios IEM reactor. The flow rate was 8 mL/min. The columns are final concentrations under 9 V (Feed = 250 ml, Pro & Bri = 100 ml; 9-h operation) and 15 V (8-h operation), and the dotted lines refer the initial concentrations of three ions in feed compartment.

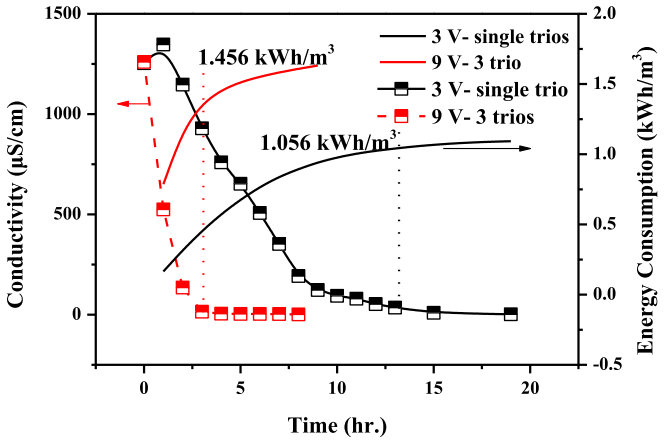

Fig. 9. The conductivity of feed compartment on the left axis and the accompanying energy consumption (kWh/m^3) on the right axis as function of time (h) when the voltages were 3 V for single trio experiment and 9 V for 3 trios experiment.

Table 4
The Comparison of single-trio IEM and 3-trios IEM experiments.

	Voltage (V)	Overall CE (%)	Electricity quantity (C)	Energy consumption (kWh/m$^{3)}$
Single–trio IEM	3	87.3	329.6	1.10
	5	90.1	333.1	1.85
	7	53.9	568.1	4.42
3-trios IEM	9	61	163.1	1.63
	15	56.7	175.2	2.92

consumption with a constant voltage as migrated current was varied with the system resistances, which is different from a constant current applied condition that previously reported [43].

As shown in Table 4, the electricity quantity was small with more trios equipped as the consumed electricity quantity was 163.1 C (E = 9 V; 3-IEM trios) compared to 329.6 C (E = 3 V; 1-IEM trio). Namely, the 3 trios experiments consumed less electric quantity. Another important parameter is the overall current efficiency (CEs), Table 4 showed the comparison of the overall current efficiency between the single-trio IEM and 3-trios IEM experiments. Since chloride, phosphate and nitrate are the anions which are considered in this experiment, the overall CEs is the sum of the CE of these three ions. The overall CEs was 87.3% (E = 3 V) in single-trio experiments, while higher than that of 61% (E = 9 V) in 3-trios experiments. This should be attribute two reasons: as the three trios reactor had 3 times average distance between two electrodes compared to the single trio reactor, and the resistance was much bigger coupled with membranes resistance. Moreover, as the three compartments of the reactor all had one inlet and water flowed successively through the stacks in 3-trios structure, the ions fluxes were much more complicated and unstable leading to a lower overall CE. However, the operating time and electricity quantity were much less than that in single trio membrane. The results indicated that the many-trios reactor is not an effective way to treat the secondary wastewater unless carefully designed to minimize resistive losses when scaling up in the future.

4. Conclusions

In this work, a novel selective electrodialysis reactor was developed in secondary wastewaters treatment for desalination and nutrients recovery. In the single-trio IEM experiment, the final conductivities of feed compartment were reaching 2 μS/cm indicating a well desalination performance. The nutrient ions of NO_3^- and HPO_4^{2-} were separated using the MVA membrane and reconcentrated in the brine and product compartment, respectively. The recovery rate increased with the increasing applied voltage, but the water dissociation took place when the voltage increased to 7 V which decreased the current efficiency and was confirmed by mathematic fitting analysis. The water dissociation got limited with a greater flow rate. The rate of desalination and nutrient reconcentration was magnified in the SED with increasing number of IEM trios and electric voltage application. The simultaneous removal of inorganic salts while selectively recovering N and P could achieve water sustainability and contribute to sustainable resource management besides obviating the risk of water pollution.

Acknowledgments

The authors wish to thank the NSFC (51508309), China Postdoctoral Science Foundation (2015M570596), the Research Award Fund for Outstanding Young Scientists of Shandong Province (BS2015HZ013), the State Key Laboratory of Microbial Technology Open Projects Fund (M2015-10) and the Fundamental Research Funds of Shandong University for the partial support of this study.

Appendix A. Supplementary data

Supplementary data associated with this article can be found, in the online version, at http://dx.doi.org/10.1016/j.cej.2017.03.149.

References

[1] K. Zuo, J. Cai, S. Liang, S. Wu, C. Zhang, P. Liang, X. Huang, A ten liter stacked microbial desalination cell packed with mixed ion-exchange resins for secondary effluent desalination, Environ. Sci. Technol. 48 (2014) 9917–9924.
[2] X. Wang, X. Zhang, Y. Wang, Y. Du, H. Feng, T. Xu, Simultaneous recovery of ammonium and phosphorus via the integration of electrodialysis with struvite reactor, J. Membr. Sci. 490 (2015) 65–71.
[3] P. Liang, L. Yuan, X. Yang, S. Zhou, X. Huang, Coupling ion-exchangers with inexpensive activated carbon fiber electrodes to enhance the performance of capacitive deionization cells for domestic wastewater desalination, Water Res. 47 (2013) 2523–2530.
[4] X. Wang, Y. Wang, X. Zhang, H. Feng, C. Li, T. Xu, Phosphate recovery from excess sludge by conventional electrodialysis (CED) and electrodialysis with bipolar membranes (EDBM), Ind. Eng. Chem. Res. 52 (2013) 15896–15904.
[5] J.A. O'Neal, T.H. Boyer, Phosphate recovery using hybrid anion exchange: applications to source-separated urine and combined wastewater streams, Water Res. 47 (2013) 5003–5017.
[6] L. Ren, Y. Ahn, B.E. Logan, A two-stage microbial fuel cell and anaerobic fluidized bed membrane bioreactor (MFC-AFMBR) system for effective domestic wastewater treatment, Environ. Sci. Technol. 48 (2014) 4199–4206.
[7] G. Qiu, Y.M. Law, S. Das, Y.P. Ting, Direct and complete phosphorus recovery from municipal wastewater using a hybrid microfiltration-forward osmosis membrane bioreactor process with seawater brine as draw solution, Environ. Sci. Technol. 49 (2015) 6156–6163.
[8] T. Tong, M. Elimelech, The global rise of zero liquid discharge for wastewater management: drivers, technologies, and future directions, Environ. Sci. Technol. 50 (2016) 6846–6855.
[9] R.P. Kralchevska, R. Prucek, J. Kolarik, J. Tucek, L. Machala, J. Filip, V.K. Sharma, R. Zboril, Remarkable efficiency of phosphate removal: Ferrate(VI)-induced in situ sorption on core-shell nanoparticles, Water Res. 103 (2016) 83–91.
[10] C. Maher, J.B. Neethling, S. Murthy, K. Pagilla, Kinetics and capacities of phosphorus sorption to tertiary stage wastewater alum solids, and process implications for achieving low-level phosphorus effluents, Water Res. 85 (2015) 226–234.
[11] B. Ebbers, L.M. Ottosen, P.E. Jensen, Electrodialytic treatment of municipal wastewater and sludge for the removal of heavy metals and recovery of phosphorus, Electrochim. Acta 181 (2015) 90–99.
[12] C.M. Werner, B.E. Logan, P.E. Saikaly, G.L. Amy, Wastewater treatment, energy recovery and desalination using a forward osmosis membrane in an air-cathode microbial osmotic fuel cell, J. Membr. Sci. 428 (2013) 116–122.
[13] W. Xue, T. Tobino, F. Nakajima, K. Yamamoto, Seawater-driven forward osmosis for enriching nitrogen and phosphorous in treated municipal wastewater: effect of membrane properties and feed solution chemistry, Water Res. 69 (2015) 120–130.
[14] F. Zaviska, P. Drogui, A. Grasmick, A. Azais, M. Héran, Nanofiltration membrane bioreactor for removing pharmaceutical compounds, J. Membr. Sci. 429 (2013) 121–129.

[15] S. Jamaly, N.N. Darwish, I. Ahmed, S.W. Hasan, A short review on reverse osmosis pretreatment technologies, Desalination 354 (2014) 30–38.
[16] S. Byun, J.S. Taurozzi, V.V. Tarabara, Ozonation as a pretreatment for nanofiltration: effect of oxidation pathway on the permeate flux, Sep. Purif. Technol. 149 (2015) 174–182.
[17] R. Kwak, G. Guan, W.K. Peng, J. Han, Microscale electrodialysis: concentration profiling and vortex visualization, Desalination 308 (2013) 138–146.
[18] M. Vaselbehagh, H. Karkhanechi, R. Takagi, H. Matsuyama, Surface modification of an anion exchange membrane to improve the selectivity for monovalent anions in electrodialysis – experimental verification of theoretical predictions, J. Membr. Sci. 490 (2015) 301–310.
[19] M.B. Kristensen, S. Haldrup, J.R. Christensen, J. Catalano, A. Bentien, Sulfonated poly(arylene thioether sulfone) cation exchange membranes with improved permselectivity/ion conductivity trade-off, J. Membr. Sci. 520 (2016) 731–739.
[20] Y. Zhang, K. Ghyselbrecht, B. Meesschaert, L. Pinoy, B. Van der Bruggen, Electrodialysis on RO concentrate to improve water recovery in wastewater reclamation, J. Membr. Sci. 378 (2011) 101–110.
[21] J. Llanos, S. Cotillas, P. Cañizares, M.A. Rodrigo, Novel electrodialysis–electrochlorination integrated process for the reclamation of treated wastewaters, Sep. Purif. Technol. 132 (2014) 362–369.
[22] A.H. Galama, G. Daubaras, O.S. Burheim, H.H.M. Rijnaarts, J.W. Post, Seawater electrodialysis with preferential removal of divalent ions, J. Membr. Sci. 452 (2014) 219–228.
[23] S. Koter, P. Chojnowska, K. Szynkiewicz, I. Koter, Batch electrodialysis of ammonium nitrate and sulfate solutions, J. Membr. Sci. 496 (2015) 219–228.
[24] M. Xie, H.K. Shon, S.R. Gray, M. Elimelech, Membrane-based processes for wastewater nutrient recovery: technology, challenges, and future direction, Water Res. 89 (2016) 210–221.
[25] B.I. Escher, W. Pronk, M.J.F. Suter, M. Maurer, Monitoring the removal efficiency of pharmaceuticals and hormones in different treatment processes of source-separated urine with bioassays, Environ. Sci. Technol. 40 (2006) 5095–5101.
[26] M. Mondor, L. Masse, D. Ippersiel, F. Lamarche, D.I. Massé, Use of electrodialysis and reverse osmosis for the recovery and concentration of ammonia from swine manure, Bioresour. Technol. 99 (2008) 7363–7368.
[27] H.J. Lee, S.J. Oh, S.H. Moon, Recovery of ammonium sulfate from fermentation waste by electrodialysis, Water Res. 37 (2003) 1091–1099.
[28] R.C. Tice, Y. Kim, Energy efficient reconcentration of diluted human urine using ion exchange membranes in bioelectrochemical systems, Water Res. 64 (2014) 61–72.
[29] B. Van der Bruggen, A. Koninckx, C. Vandecasteele, Separation of monovalent and divalent ions from aqueous solution by electrodialysis and nanofiltration, Water Res. 38 (2004) 1347–1353.
[30] Y. Zhang, E. Desmidt, A. Van Looveren, L. Pinoy, B. Meesschaert, B. Van der Bruggen, Phosphate separation and recovery from wastewater by novel electrodialysis, Environ. Sci. Technol. 47 (2013) 5888–5895.
[31] A.T.K. Tran, Y. Zhang, D. De Corte, J.-B. Hannes, W. Ye, P. Mondal, N. Jullok, B. Meesschaert, L. Pinoy, B. Van der Bruggen, P-recovery as calcium phosphate from wastewater using an integrated selectrodialysis/crystallization process, J. Cleaner Prod. 77 (2014) 140–151.
[32] C.D. Nezungai, T. Majozi, Optimum synthesis of an electrodialysis framework with a background process—I: a novel electrodialysis model, Chem. Eng. Sci. 147 (2016) 180–188.
[33] H. Yan, C. Xu, W. Li, Y. Wang, T. Xu, Electrodialysis to concentrate waste ionic liquids: optimization of operating parameters, Ind. Eng. Chem. Res. 55 (2016) 2144–2152.
[34] C.V. Gherasim, J. Křivčík, P. Mikulášek, Investigation of batch electrodialysis process for removal of lead ions from aqueous solutions, Chem. Eng. J. 256 (2014) 324–334.
[35] R. Takagi, M. Vaselbehagh, H. Matsuyama, Theoretical study of the permselectivity of an anion exchange membrane in electrodialysis, J. Membr. Sci. 470 (2014) 486–493.
[36] S. Abdu, M.C. Marti-Calatayud, J.E. Wong, M. Garcia-Gabaldon, M. Wessling, Layer-by-layer modification of cation exchange membranes controls ion selectivity and water splitting, ACS Appl. Mater. Interfaces 6 (2014) 1843–1854.
[37] T. Kikhavani, S.N. Ashrafizadeh, B. Van der Bruggen, Nitrate selectivity and transport properties of a novel anion exchange membrane in electrodialysis, Electrochim. Acta 144 (2014) 341–351.
[38] Y. Zhang, S. Paepen, L. Pinoy, B. Meesschaert, B. Van der Bruggen, Selectrodialysis: Fractionation of divalent ions from monovalent ions in a novel electrodialysis stack, Sep. Purif. Technol. 88 (2012) 191–201.
[39] H. Strathmann, A. Grabowski, G. Eigenberger, Ion-exchange membranes in the chemical process industry, Ind. Eng. Chem. Res. 52 (2013) 10364–10379.
[40] L. Alvarado, A. Chen, Electrodeionization: principles, strategies and applications, Electrochim. Acta 132 (2014) 583–597.
[41] V.V. Nikonenko, N.D. Pismenskaya, E.I. Belova, P. Sistat, P. Huguet, G. Pourcelly, C. Larchet, Intensive current transfer in membrane systems: modelling, mechanisms and application in electrodialysis, Adv. Colloid Interface Sci. 160 (2010) 101–123.
[42] R.D. Patel, K.-C. Lang, I.F. Miller, Polarization in ion-exchange membrane electrodialysis, Ind. Eng. Chem. Fund. 16 (1977) 340–348.
[43] A.H. Galama, G. Daubaras, O.S. Burheim, H.H.M. Rijnaarts, J.W. Post, Fractioning electrodialysis: a current induced ion exchange process, Electrochim. Acta 136 (2014) 257–265.